



## Coordination polymer-derived CuO catalysts for oxidative degradation of methylene blue



O.J. Silva Junior<sup>a</sup>, A.F.F. Monteiro<sup>b</sup>, J.B.L. Oliveira<sup>a</sup>, A.M.U. Araújo<sup>c</sup>, D.G. Silva<sup>d</sup>, J. Kulesza<sup>b,\*\*</sup>, B.S. Barros<sup>e,\*</sup>

<sup>a</sup> Universidade Federal do Rio Grande do Norte, Instituto de Química, 59064-741, Natal, RN, Brazil

<sup>b</sup> Universidade Federal de Pernambuco, Departamento de Química Fundamental, 50740-540, Recife, PE, Brazil

<sup>c</sup> Universidade Federal do Rio Grande do Norte, Escola de Ciência & Tecnologia, 59078-970, Natal, RN, Brazil

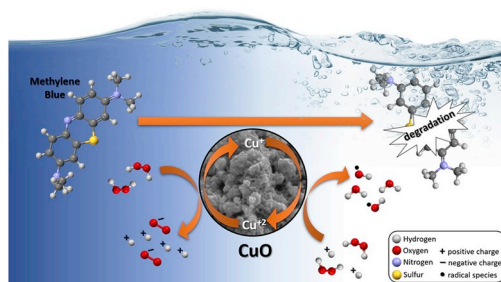
<sup>d</sup> Instituto Federal de Educação, Ciência e Tecnologia do Rio Grande do Norte, Campus Zona Norte, 59112-490, Natal, RN, Brazil

<sup>e</sup> Universidade Federal de Pernambuco, Departamento de Engenharia Mecânica, 50740-550, Recife, PE, Brazil

### HIGHLIGHTS

- Cu-coordination polymers (Cu-CPs) were prepared via rapid electrochemical method.
- CP-derived CuO were successfully obtained via one-step calcination process.
- Prepared CuO showed excellent catalytic degradation properties of methylene blue.
- Effect of catalyst and H<sub>2</sub>O<sub>2</sub> contents on discoloration process was studied.

### GRAPHICAL ABSTRACT



### ARTICLE INFO

#### Keywords:

CuO  
Coordination polymers  
Methylene blue  
H<sub>2</sub>O<sub>2</sub>  
Degradation

### ABSTRACT

Coordination polymers (CP) are a new class of hybrid materials consisting of metal clusters connected by organic ligands and forming structures along one, two or three dimensions. Three Cu<sup>2+</sup> coordination polymers Cu(1,3-BDC)·3H<sub>2</sub>O, Cu(1,4-BDC), and Cu(5-NH<sub>2</sub>-1,3-BDC) (BDC = benzenedicarboxylic) were prepared via an electrochemical method and used as precursors for CuO by calcination in air at 650 °C. All the prepared samples were characterized by Powder X-ray Diffraction (PXRD), Attenuated Total Reflectance Fourier Transform Infrared spectroscopy (ATR-FTIR), Thermal Analysis (TGA-DTA), and Scanning Electron Microscopy (SEM). The results confirmed both the crystallization of the CPs and the formation of copper oxide after the thermal treatment. The CP-derived CuO was tested in the catalytic degradation of the methylene blue in the presence of H<sub>2</sub>O<sub>2</sub>, and the effect of reaction parameters such as the mass of catalyst and volume of H<sub>2</sub>O<sub>2</sub> were studied. Cu(1,4-BDC)-derived CuO catalyst showed discoloration efficiency about 92% at 308 K, and 100% at 331 K after 120 and 30 min, respectively with good recyclability up to the four cycles (71.77%).

\* Corresponding author.

\*\* Corresponding author.

E-mail addresses: [joanna.kulesza@ufpe.br](mailto:joanna.kulesza@ufpe.br) (J. Kulesza), [braulio.barros@ufpe.br](mailto:braulio.barros@ufpe.br) (B.S. Barros).

## 1. Introduction

The availability of fresh water is crucial to the survival of all living beings including the human species [1]. Although 70% of the earth's surface is mainly composed of water, only 3% of this water is fresh, with just 1% being accessible for human consumption [2]. Besides, water effluents contamination by industrial chemical raw materials like organic dyes has become a severe environmental worldwide problem in the last decades [1,3,4]. Organic dyes are used in a wide range of industrial activities and products such as plastic, paint, paper, pharmaceuticals, cosmetics, and ornaments to give a few examples [1,4]. One of the most known and used organic dyes is the methylene blue (MB), a cyclic compound with a chemical formula  $C_{16}H_{18}N_3S^+$  which in aqueous medium produces  $C_{16}H_{18}N_3S^+$  cations. Dyes like MB are usually tricky to degrade because they are very stable to light, heat and oxidation reactions [5,6]. Physical, chemical and biological methods have been proposed for the removal of organic dyes from contaminated water [1,5]. Some of the chemical methods include techniques like coagulation/flocculation, oxidation processes and ion exchange [3,7].

Most recently, the catalytic oxidation of organic dyes in the presence of metal oxides and hydrogen peroxide ( $H_2O_2$ ) has been considered as an efficient, low-cost and straightforward alternative to treat contaminated effluents [3,8]. Hydrogen peroxide is a weak acid with strong oxidizing character and environmentally friendly nature once its decomposition produces water and oxygen [9]. However, in the presence of NaOH,  $H_2O_2$  generates free radical species like  $HO\bullet$ ,  $HOO\bullet$  or  $O_2\bullet$ . These radicals, especially  $HO\bullet$ , present stronger oxidant properties than the  $H_2O_2$  [9]. The oxidation processes involving the generation of hydroxyl radicals ( $HO\bullet$ ) are known as Advanced Oxidation Processes (AOPs). Very often these reactions take place with the help of a catalyst, such as  $Fe^{+2}/Fe^{+3}$  ions, Fenton process [8,10,11], or  $Cu^+/Cu^{+2}$  ions, cupro-Fenton process [12]. In these cases, the catalyst works together with hydroxyl radicals degrading a wide variety of compounds, such as methylene blue [4,13], methyl orange [14], alcohol [15], trichloroethylene [16], surfactants [17], wood [18], *N,N*-diethyl-*p*-phenylenediamine [19], benzene, toluene, ethylbenzene and xylenes [20], and chlorine-substituted disinfectants [21]. Metal oxides such as  $TiO_2$ ,  $Fe_3O_4$ ,  $SnO_2$ , and CuO are good examples of catalysts for AOPs, specially CuO, due to its low cost, high efficiency, and environmental stability [3].

The cupric oxide (CuO) is a p-type semiconductor with a narrow band gap (1.2–1.5 eV) widely used in catalysis, ion exchange, sensors, and environmental treatment [4,9]. The small band gap is especially interesting for photocatalytic applications using sunlight [9]. Its photocatalytic properties are related to the presence of  $Cu^+/Cu^{+2}$  species which allow the oxidative transformations of organic compounds [9]. Besides that, the general properties of CuO powders are dependent on its morphological characteristics, mainly surface area, and porosity. Therefore, the development of new synthetic approaches that allow the tailoring of the micro/nanostructure of the catalysts is still a challenge.

Many methods have been used to prepare CuO, solution combustion [9], hydrothermal [22–24], ultrasound [25], double-jet precipitation [26] and most recently via thermal decomposition of Metal-Organic Frameworks (MOFs) [27–30]. The use of MOFs as precursors is a promising alternative to the preparation of catalysts used in the degradation of various substances. MOFs are classified as 2D or 3D coordination polymers with an intrinsic porous structure. They usually have a high surface area and a large volume of pores, which make them attractive materials for applications in catalysis, adsorption, separation, and gas storage [5,31–33]. Interestingly, these properties may be inherited by the oxides prepared via thermal decomposition of porous coordination polymers.

In this work, the cupric oxide was successfully prepared via thermal decomposition of Cu-based CPs synthesized by an electrochemical method. Three different organic ligands were used in the synthesis of CPs, 1,3- $H_2BDC$ , 1,4- $H_2BDC$ , and 5- $NH_2-H_2BDC$ . The obtained CuO powders were used as catalysts in the degradation of methylene blue in the

presence of  $H_2O_2$ .

## 2. Experimental

### 2.1. Materials and synthesis

All reagents were used as received, without further purification. Isophthalic acid (1,3- $H_2BDC$ , 99%), terephthalic acid (1,4- $H_2BDC$ , 99%) and aminoisophthalic acid (5- $NH_2-1,3-H_2BDC$ , 94%) were purchased from Sigma-Aldrich. Sodium nitrate ( $NaNO_3$ , 99.5%), ethanol ( $C_2H_5OH$ , 99.5%), *N,N*-dimethylformamide (DMF,  $C_3H_7NO$ ), hydrogen peroxide ( $H_2O_2$ , 30%), and methylene blue trihydrate (MB,  $C_{16}H_{18}N_3S \cdot 3H_2O$ ) were acquired from Atrium, VETEC, Dynamic, ISOFAR, and IMPEX, respectively. Copper metal wires with a purity of 99.95% were used as metal ions source.

The CPs were prepared by an electrochemical method following the methodology described in the literature [34–36]. In a typical procedure, 1 g (6.02 mmol) of 1,3- $H_2BDC$  was dissolved in 40 mL of DMF (solution A), and 0.60 g (7.06 mmol) of  $NaNO_3$  in 40 mL of distilled water (solution B). The solutions A and B were mixed in an electrochemical cell and the resultant solution kept under constant magnetic stirring at room temperature. Then, two copper electrodes were immersed in the solution, and a voltage of 10 V applied between them for 1 h. During this time the formation of a precipitate of CP1 was observed. The samples CP2 and CP3 were prepared following the same procedure but changing the organic ligand to 1,4- $H_2BDC$  and 5- $NH_2-1,3-H_2BDC$ , respectively. The produced samples were collected by centrifugation (5 min at 3600 rpm), washed with a solvent and again centrifugated. This procedure was repeated three times using DMF and distilled water alternately. Finally, the samples were dried in an oven at 60 °C for 3 h.

CuO powders were prepared via thermal decomposition of the coordination polymers. The samples CP1, CP2, and CP3 were calcined at 650 °C for 3 h to produce samples CU1, CU2, and CU3, respectively.

### 2.2. Sample characterization

The prepared samples were characterized by Scanning Electron Microscopy (SEM) in TESCAN equipment model VEGA3, operating at 15 kV. X-ray Powder Diffraction (XRPD) analyses were performed in a Bruker D2 Phaser equipment working with  $Cu-K\alpha$  radiation ( $\lambda_{Cu} = 1.542 \text{ \AA}$ ). Thermal Gravimetric Analysis (TGA) was conducted on a Shimadzu DTG-60H thermal analysis system. The samples were heated from 30 to 900 °C at a rate of 10 °C/min<sup>-1</sup> under nitrogen atmosphere. Attenuated Total Reflectance Fourier Transform Infrared (ATR-FTIR) spectroscopy analyses were carried out using a Bruker Vertex 70/v spectrometer.

### 2.3. Determination of the catalytic activity of CP-derived CuO

The catalytic activity of MOF-derived CuO samples was evaluated for the oxidation of methylene blue (MB) in the presence of hydrogen peroxide in aqueous solution. In these experiments, 2.5 mL of 30%  $H_2O_2$ , 10 mL of the methylene blue solution (60.0  $\mu\text{mol L}^{-1}$ ) and 20 mg of CuO were mixed at room temperature and kept under constant magnetic stirring for 150 min. After that time, the supernatant was centrifuged, and the remaining MB concentration was determined using the absorbance values measured at 665 nm from the UV–Vis spectra. The absorbance values were converted to MB concentration values using a calibration curve (see Fig. S1). Five standard solutions with pH 5.6 and 1, 2, 3, 4 and 5 ppm of MB were prepared. Then, the UV–Vis spectra of these solutions were acquired, and the respective absorbance values at 665 nm used to build the calibration curve. All experiments were performed in a Biospectro UV spectrophotometer model SP-220.

All tests were performed at pH 5.6, which was determined as the best pH at which maximum MB discoloration occurred. The experiments of the influence of pH on discoloration efficiency were performed using

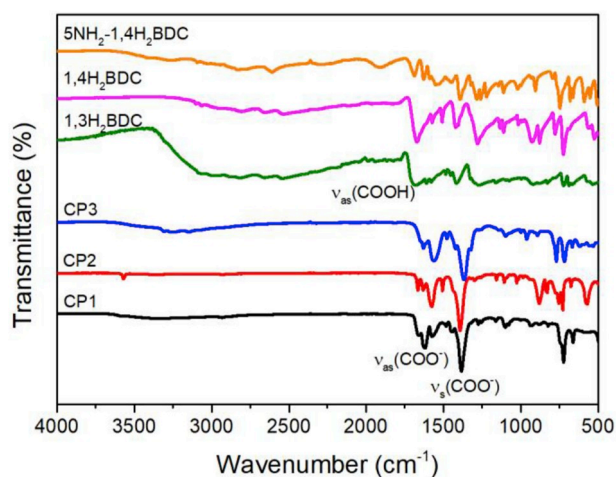


Fig. 1. FTIR-ATR spectra of the coordination polymers and the pure organic ligands.

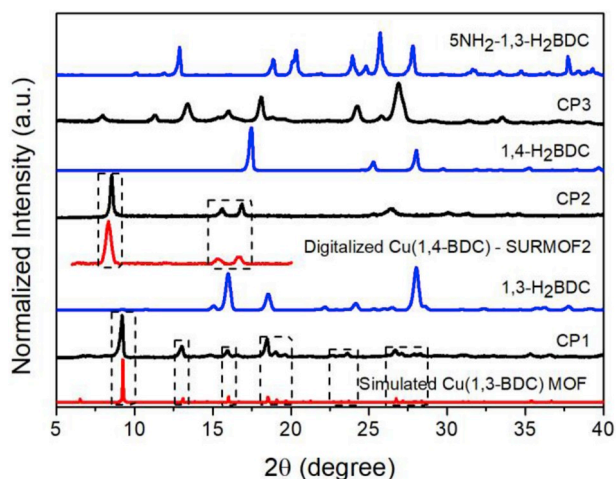


Fig. 2. PXRD patterns of the coordination polymers (experimental and digitalized/simulated) and pure organic ligands (experimental).

10 mL of the aqueous solution of MB ( $60.0 \mu\text{mol L}^{-1}$ ) in the presence of 2.0 mL of 30%  $\text{H}_2\text{O}_2$ , and 20 mg of a representative sample (CU2) at room temperature and under constant magnetic stirring for 90 min. The pH of the solutions was fixed at 2.6, 3.6, 5.6, 8.4 or 9.5 by adding the appropriate amount of HCl or NaOH. The maximum of MB discoloration was achieved at pH 5.6 (Fig. S2). Thus, this pH value was chosen for further studies.

### 3. Results and discussions

#### 3.1. Coordination polymers (CPs)

ATR-FTIR spectra of the samples CP1, CP2 and CP3 and of the pure ligands (1,3- $\text{H}_2\text{BDC}$ , 1,4- $\text{H}_2\text{BDC}$ , 5- $\text{NH}_2$ -1,4- $\text{H}_2\text{BDC}$ ) are depicted in Fig. 1. In the spectra of the samples CP1, CP2 and CP3, no bands in the region of  $1680\text{--}1730 \text{ cm}^{-1}$  are visible what indicates the complete deprotonation of the respective carboxylic acid and coordination of the  $\text{COO}^-$  groups to the copper center. The band centered at approximately  $3200 \text{ cm}^{-1}$  is attributed to the stretching  $\nu$  (N-H) vibration of the primary amine group suggesting the presence of uncoordinated  $\text{NH}_2$  moiety in the sample of CP3. Moreover, the bands at 1665 (more evident for CP1 and CP2) and  $3338 \text{ cm}^{-1}$  for CP1 (and less intense for CP2) may be attributed to the stretching  $\nu$  (C=O) and (O-H) vibrations of the

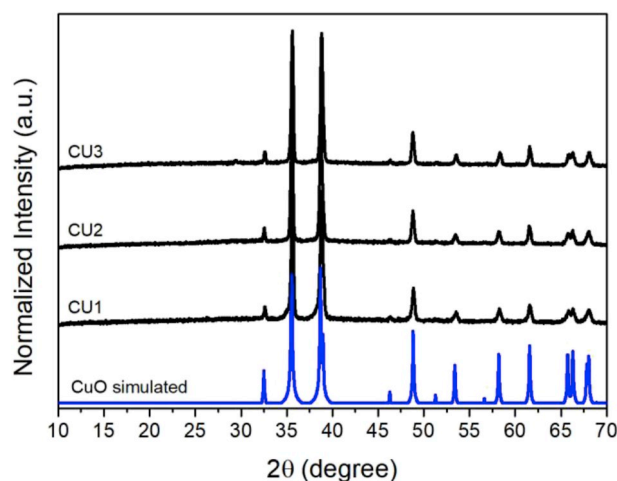


Fig. 3. PXRD patterns of the CuO samples.

coordinated DMF and water, respectively, present in the structures.

The produced samples were characterized by powder X-ray diffraction technique to confirm the crystallinity and identify the phases formed. The diffractograms of the coordination polymers and the pure ligands are shown together with the reference patterns (simulated and digitalized) in Fig. 2. The diffraction patterns of the samples CP1, CP2, and CP3 do not match with the patterns of the correspondent pure ligands, what corroborates with ATR-FTIR results and suggests the crystallization of metal-organic structures.

The diffractogram of CP1 matches well with the simulated pattern of the coordination polymer  $\text{Cu}(1,3\text{-BDC})\cdot 3\text{H}_2\text{O}$  (CCDC CIF file n° 247686). This CP crystallizes with a tetragonal symmetry, space group  $\text{P4/n}$ , displaying a layered structure stacked along the  $c$  axis. In the layers, the copper atoms form paddle-wheel clusters coordinated by four 1,3-BDC molecules along the plane perpendicular to the  $c$  axis, and two water molecules in the apical positions. Each 1,3-BDC molecule coordinate two paddle-wheel clusters. It is worth noting that, the stacking of the layers give rise to channels along the  $c$  axis, which accommodate water molecules [35,37]. The diffraction pattern of CP2 presents the same set of peaks observed in the diffractogram of the coordination polymer  $\text{Cu}(1,4\text{-BDC})$  termed SURMOF-2, previously reported by Liu and co-workers [38]. The structure of CP2 presents a regular packing of  $(\text{Cu}^{+2})_2$ -carboxylate paddle-wheel planes with  $\text{C}_2$  symmetry [38]. Unfortunately, it was not possible to identify the crystalline structure of CP3. However, its diffraction pattern does not match with that from the pure ligand suggesting the crystallization of a new phase, probably a metal-organic structure.

Thermal gravimetric analysis (TGA) was performed to study the stability of the CPs (Fig. S3). Three distinct weight losses were observed for the sample CP1 at  $30\text{--}190$ ,  $190\text{--}280$  and  $280\text{--}400 \text{ }^\circ\text{C}$ . The first step of decomposition is related to the desorption of solvent molecules present in the pores, also observed for the sample CP3. The second step associated with the desorption of solvent molecules coordinated to the metal sites was also noted for the sample CP2. Finally, the third step is related to the organic ligand decomposition leading to the oxide formation, also observed for both CP2 and CP3. However, the temperature of the transformation of PCs into copper oxide is slightly different for each precursor ( $400$ ,  $550$  and  $500 \text{ }^\circ\text{C}$  for CP1, CP2, and CP3, respectively) what may be related to the different organic ligand present in these structures. It is worth noting, by choosing the appropriate organic ligand, the minimum temperature needed for the calcination may be controlled.

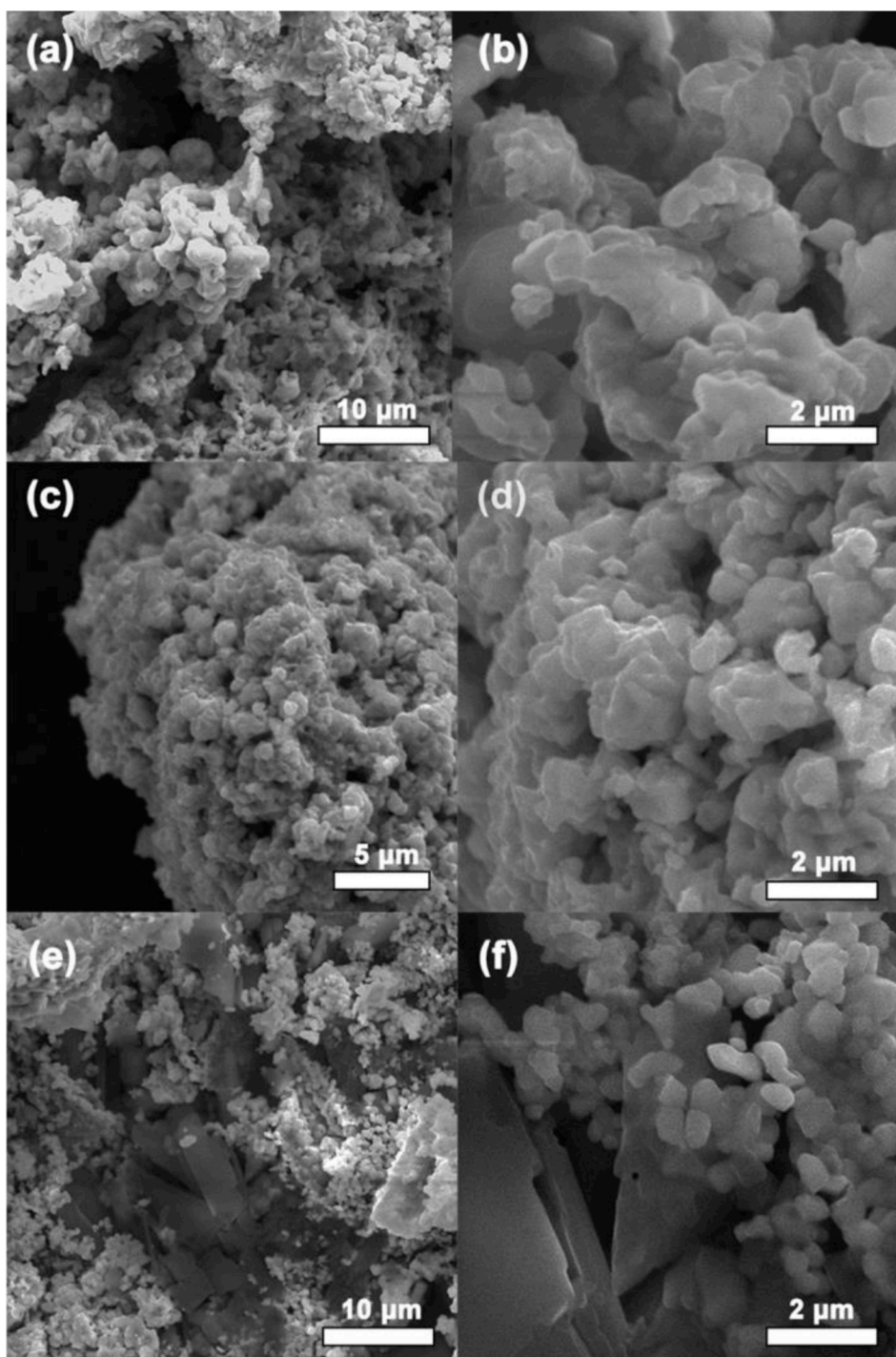


Fig. 4. SEM images of the samples CU1 (a)–(b), CU2 (c)–(d) and CU3 (e)–(f).

### 3.2. CuO

To ensure the complete decomposition of the precursors, the temperature of 650 °C was chosen for the calcination.

Fig. 3 shows the diffractograms of the samples CU1, CU2, and CU3, obtained from the calcinated coordination polymers. As can be seen, the diffraction peaks of the three samples match well with the simulated pattern of CuO with the Tenorite structure (COD CIF file n° 9015924). No secondary crystalline phases were observed.

To investigate the microstructural characteristics of the obtained CuO powders, SEM analyses were performed. The micrographs are presented in Fig. 4. Samples CU1 and CU2 exhibit irregular porous

agglomerates formed by submicrometric particles. These particles are clearly in an intermediate sintering stage. However, it is worth noting that CU1 seems to be in a more advanced step of sintering compared to the other samples. On the other hand, the sample CU3 exhibit two distinct microstructures, irregular submicrometer particles, and plates with a smooth surface. These submicrometer particles appear to be in an initial step of sintering, unlike what was observed in other samples. It is possible that the presence of a second microstructure retarded the particle sintering effects. These results also suggest that the crystalline structure of the CPs may influence the microstructural characteristics of the oxides produced via thermal decomposition.

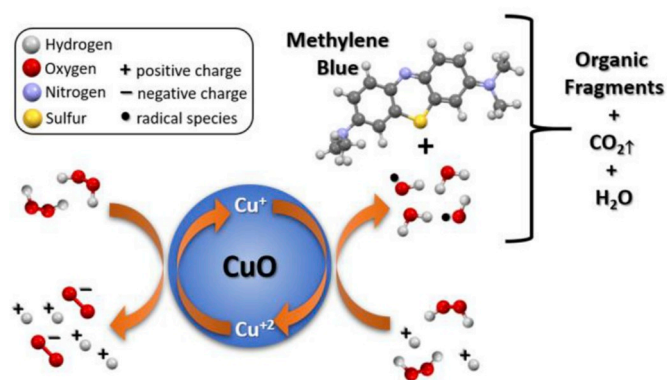
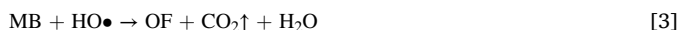


**Fig. 5.** Schematic representation of the mechanism involved in the degradation of methylene blue in the presence of  $\text{H}_2\text{O}_2$ . (For interpretation of the references to color in this figure legend, the reader is referred to the Web version of this article.)

### 3.3. Catalytic degradation of methylene blue

The Cupro-Fenton is an alternative to conventional Fenton-like reactions using  $\text{Fe}^{2+}/\text{Fe}^{3+}$  ions [8,10,11].  $\text{Cu}^+/\text{Cu}^{2+}$  ions are used as catalysts together with  $\text{H}_2\text{O}_2$  to degrade various organic substances such as dyes [3,4,9]. It is well accepted that the decomposition of  $\text{H}_2\text{O}_2$  takes place over the surface of  $\text{CuO}$  particles (Fig. 5). The  $\text{Cu}^+/\text{Cu}^{2+}$  pair activates the hydrogen peroxide molecules (equations (1) and (2)), generating hydroxyl radicals ( $\text{HO}\bullet$ ) [39,40]. Finally, the hydroxyl radicals degrade methylene blue molecules (MB) forming organic fragments (OF) [19].



The discoloration values of MB are shown in Fig. 6a. The samples CU2 and CU3 exhibited the best results, 86%, and 85%, respectively, compared to 45% for sample CU1. Therefore, samples CU2 and CU3

were selected for further investigations.

The effect of the catalyst mass on the discoloration of MB was evaluated, and the results are exhibited in Fig. 6b. As expected, by increasing the catalyst mass, and so the number of active sites for  $\text{H}_2\text{O}_2$  decomposition, the discoloration efficiency also increases, reaching values around 84–86% for 20 mg of catalyst. Tests performed with 25 mg of catalyst exhibited similar results, suggesting that the catalyst excess does not play a significant role in the process. According to Tabai and co-workers [41], the catalyst excess may promote side reactions that consume hydroxyl radicals. It is also possible that a higher amount of catalyst leads to the aggregation of particles and decreasing the number of surface active sites [42].

The effect of  $\text{H}_2\text{O}_2$  concentration on the discoloration of MB in the presence of CU2 catalyst is illustrated in Fig. 6c. The results indicated that lower  $\text{H}_2\text{O}_2$  volume (2.0 mL) promoted higher discoloration efficiency. When the concentration of  $\text{H}_2\text{O}_2$  in a solution is too high, the hydrogen peroxide molecules react with hydroxyl radicals to form hydroperoxyl radicals ( $\text{HOO}\bullet$ ), which presents a much lower oxidation potential compared to the  $\text{HO}\bullet$  radical [41,43]. It was found that  $\text{H}_2\text{O}_2$  should be added at an optimum concentration to assure the best degradation performance, in our case 2.0 mL.

The degradation kinetics of MB was evaluated based on the respective concentration profiles. The experiments were conducted at three different temperatures (308, 318 and 331 K) for 120 min by using 6.25 mL of 30%  $\text{H}_2\text{O}_2$ , 25 mL of the methylene blue solution ( $718.0 \mu\text{mol L}^{-1}$ ) and 50 mg of the CU2 catalyst. The obtained data were adjusted to zero-order, pseudo-first-order, and pseudo-second-order kinetic models by using the following equations:

$$C_t - C_0 = -k_0t \quad [4]$$

$$C_t / C_0 = e^{-k_1t} \quad [5]$$

$$(1/C_t) - (1/C_0) = k_2t \quad [6]$$

where  $C_0$  and  $C_t$  are the MB concentrations ( $\text{mgL}^{-1}$ ) at the initial time and reaction time  $t$ , and  $k_0$ ,  $k_1$  and  $k_2$  are the zero-order rate constant ( $\text{mgL}^{-1}\text{min}^{-1}$ ), the pseudo-first-order rate constant ( $\text{min}^{-1}$ ) and the pseudo-second-order rate constant ( $\text{Lmg}^{-1}\text{min}^{-1}$ ), respectively.

The best fit was achieved when a model of pseudo-first-order was

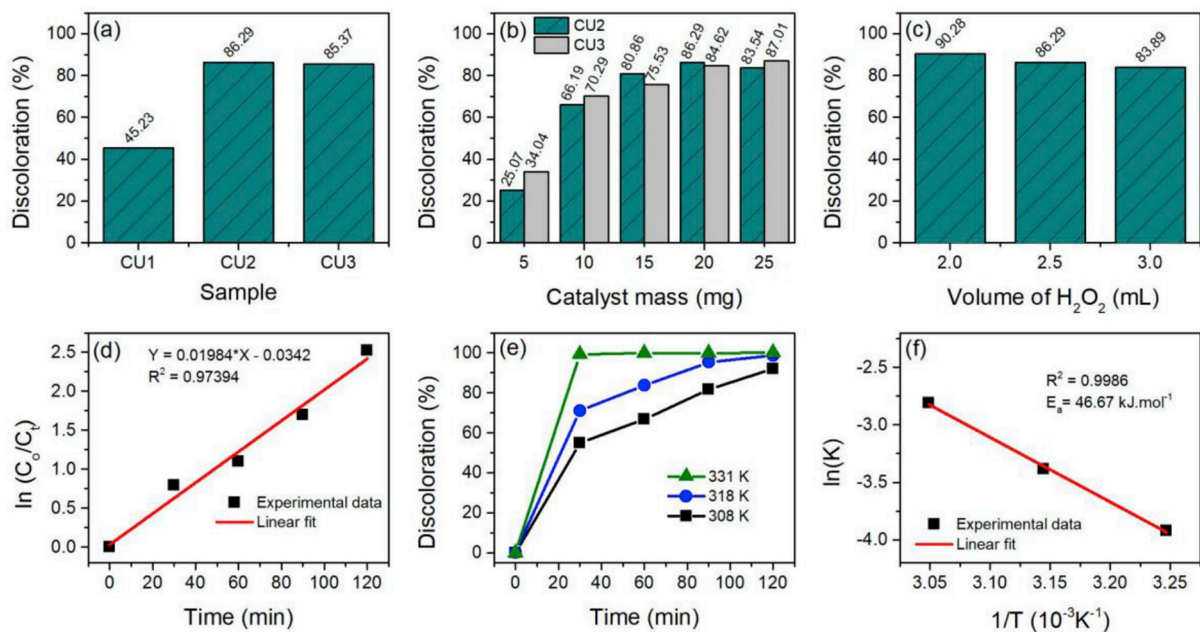


**Fig. 6.** (a) Discoloration efficiency of the tested catalysts; (b) Effect of the catalyst mass; (c) Effect of the  $\text{H}_2\text{O}_2$  volume; (d) Plot of  $\ln(C_0/C_t)$  versus time; (e) Effect of the temperature on the discoloration of MB as a function of time; (f) Plot of  $\ln(K)$  versus  $1/T$  in the temperatures of 308, 318 and 331 K.

**Table 1**

The linear correlation coefficients and the rate constants for the catalytic oxidation of the MB using the sample CU2 and considering zero-order, pseudo-first-order and pseudo-second-order kinetic models under the following conditions: 6.25 mL of 30% H<sub>2</sub>O<sub>2</sub>, 25 mL of a solution with 718 μmol L<sup>-1</sup> of MB and 50 mg of catalyst.

	zero-order			pseudo-first-order			pseudo-second-order		
Temp. (K)	308	318	331	308	318	331	308	318	331
R <sup>2</sup>	0.8605	0.7484	0.5057	0.9805	0.9892	0.8594	0.8202	0.7416	0.7573
t <sub>1/2</sub> (min)	-	-	-	35.00	20.44	11.65	-	-	-
k <sup>a</sup>	5.0503	5.2984	4.8048	0.0198	0.0339	0.0602	1 × 10 <sup>-4</sup>	7 × 10 <sup>-4</sup>	0.0308

<sup>a</sup> Zero-order μmol.L<sup>-1</sup>. min<sup>-1</sup>; pseudo-first-order min<sup>-1</sup>; pseudo-second-order L.μmol<sup>-1</sup>. min<sup>-1</sup>.

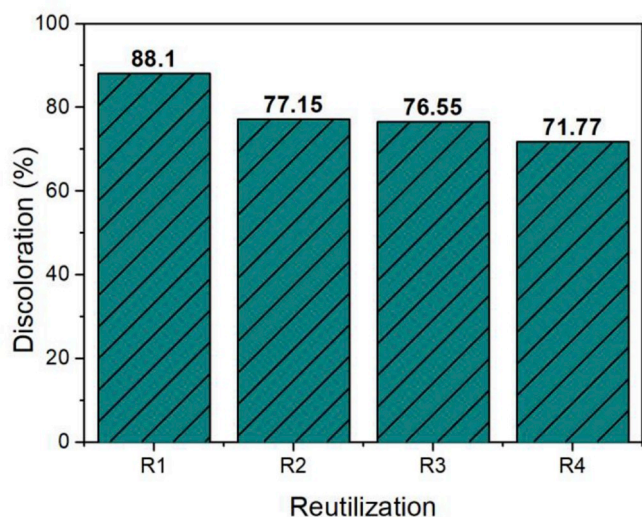


**Fig. 7.** Effect of recycling number on the discoloration of MB (10 mL, 60.0 μmol L<sup>-1</sup>) in the presence of 2.0 mL of 30% H<sub>2</sub>O<sub>2</sub>, and 20 mg of CU2 at room temperature for 90 min.

used, what is in agreement with the model postulated by Prathap and coworkers [44]. Fig. 6d exhibits the plot of ln(C<sub>0</sub>/C<sub>t</sub>) as a function of time for the CU2 catalyst. As can be seen, the data collected at 308 K throughout 120 min presents a good linear correlation (R<sup>2</sup> = 0.9805) and a pseudo-first-order rate constant (k<sub>1</sub>) of 0.01984 min<sup>-1</sup>. On the other hand, the values of linear correlation for zero-order, and pseudo-second-order models were lower (see Table 1), suggesting that the degradation reaction follows the first-order kinetics with respect to MB.

Fig. 6e displays discoloration efficiency as a function of time, which reached about 92% at 308 K after 120 min, with a half-life of 35 min. It is

worth noting that at higher temperatures, the efficiency increases and reaches 100% at 331 K after only 30 min. The slope of the plot ln(K) versus 1/T gave the activation energy (E<sub>a</sub>) of 46.67 kJ mol<sup>-1</sup> (see Fig. 6f).

The sample CU2 was recovered and reused to investigate the stability of the CuO in the catalytic oxidation of MB. The recovered sample was recycled four times for experiments of MB degradation. At the end of each cycle, the catalyst was washed with ethanol three times followed by drying in an oven. The tests for reusability were performed using 10 mL of the aqueous solution of MB (60.0 μmol L<sup>-1</sup>) in the presence of 2.0 mL of 30% H<sub>2</sub>O<sub>2</sub>, and 20 mg of CU2 at room temperature and under constant magnetic stirring for 90 min. The initial percentage of discoloration (88.10) only decreased to 77.15, 76.55 and 71.77% after, two, three, and four cycles, respectively, confirming good recyclability up to four cycles (Fig. 7).

The kinetic parameters for the catalytic degradation of methylene blue using CU2 catalyst were compared with those achieved over other CuO catalysts reported in the literature (Table 2).

MOF-derived CuO reported in this work presents higher reaction rate of the catalytic degradation of methylene blue (k = 1.98 × 10<sup>-2</sup> min) at near ambient temperature (308 K) when compared to other CuO structures reported in the literature; k = 1.30 (298 K) [4], 0.91 (308 K) [40], 0.71 (308 K) [40], and k < 0.37 × 10<sup>-2</sup> min (298 K) [45]. Also, the activation energy is lower than for the above cited CuO catalysts.

As observed in Fig. 5e, the discoloration efficiency reached about 92% at 308 K after 2 h (50% after only 35 min), and 100% at 331 K after only 30 min. Although CuO nanosheets reported by Zhu et al. demonstrated 96.5% efficiency after 15 min at ambient temperature, the discoloration efficiency dropped fast after second (62.3%) and third (33.5%) recycle number [4], whereas our catalyst retained 76.55% efficiency after third recycle. Deka et al. reported the degradation efficiency of MB at 338 K equal to 100% after 25 and 35 min, for sheet-like CuO and rectangle-like CuO blocks, respectively [40]. These results are similar to our data for experiments carried out at 308 K, although our catalyst promotes lower activation energy than CuO nanostructures

**Table 2**

Comparison of the kinetic parameters for the catalytic degradation of MB over different CuO catalysts.

Sample	Temp. (K)	k × 10 <sup>-2</sup> (min <sup>-1</sup> )	k (h <sup>-1</sup> )	E <sub>a</sub> (kJ.mol <sup>-1</sup> )	Condition	Ref.
CU2	308	1.98	1.188	46.67	50 mg catalyst	This work
	318	3.39	2.034		6.25 mL (30% H <sub>2</sub> O <sub>2</sub> )	
	331	6.02	3.612		50 mL (718.0 μmol L <sup>-1</sup> or 268.1 mg L <sup>-1</sup> MB)	
CuO nanosheets	298	1.30	0.780	54.0	20 mg catalyst 2.5 mL (30% H <sub>2</sub> O <sub>2</sub> ) 10 mL (60.0 μmol L <sup>-1</sup> MB)	[4]
Sheet-like CuO	298	0.22	0.132	64.53	3.0 mg catalyst	[40]
	308	0.91	0.546		1 mL (30% H <sub>2</sub> O <sub>2</sub> )	
	338	9.24	5.444		10 mL (5.0 mg L <sup>-1</sup> MB)	
Rectangle-like CuO blocks	298	0.21	0.126	71.87		
	308	0.71	0.426			
	338	6.99	4.194			
Plate-like CuO	298	0.37	0.226	<sup>a</sup>	20.0 mg catalyst	[45]
Flower-like CuO		0.32	0.192		20 mL (30% H <sub>2</sub> O <sub>2</sub> )	
Boat-like CuO		0.33	0.197		100 mL (10.0 mg L <sup>-1</sup> MB)	
Ellipsoid-like CuO		0.26	0.155			
Commercial CuO		0.23	0.135			

<sup>a</sup> Not informed.

reported by Deka et al. The efficiency of our catalyst in discoloration of MB is also much higher than for CuO nanostructures reported by Yang et al. [45]. High degradation levels were reached only after 10 h (97.2%, 96.0%, and 96.1% for plate-like, flower-like, and boat-like CuO, respectively), while ellipsoid-like CuO and commercial CuO, reached only 89.7% and 80.1% after this time [45].

#### 4. Conclusion

CuO powders were successfully obtained by the thermal decomposition of three copper-based coordination polymers (CPs). The catalytic activity of the oxide samples was evaluated over the oxidation of methylene blue (MB) with hydrogen peroxide in aqueous solution. The CuO powders prepared from the CP precursors containing the organic ligands 1,4-H<sub>2</sub>BDC and 5-NH<sub>2</sub>-H<sub>2</sub>BDC presented the highest discoloration values, about 86 and 85% at room temperature, respectively. It appears that the type of the organic ligand and the crystalline structure of the CP have a significant influence on the microstructure of the oxide-products obtained by thermal decomposition. CuO derived from Cu(1,3-BDC).3H<sub>2</sub>O presented a microstructure with agglomerates in a more advanced step of sintering compared to samples obtained by thermolysis of Cu(1,4-BDC), and Cu(5-NH<sub>2</sub>-1,3-BDC), which may imply in less available active catalytic sites and lower degradation efficiency in the first case (45.23 vs 86.29, and 85.37%, respectively). For the optimal reaction conditions, 20 mg of catalyst and 2 mL of H<sub>2</sub>O<sub>2</sub> 30%, the discoloration efficiency presented by sample Cu(1,4-BDC)-derived CuO reached about 92 and 100% at 308 and 331 K, respectively with good recyclability up to the four cycles (71.77%). In summary, CuO catalysts prepared by decomposition of CPs exhibited promising properties for the discoloration of dyes in water.

#### Acknowledgments

The authors thank the Brazilian agencies CNPq and FACEPE (CNPq Grant no. 407445/2013-7 and PRONEX/FACEPE/CNPq Grant no. APQ-0675-1.06/14).

#### Appendix A. Supplementary data

Supplementary data to this article can be found online at <https://doi.org/10.1016/j.matchemphys.2019.121737>.

#### References

- X. Liu, J. Luo, Y. Zhu, Y. Yang, S. Yang, Removal of methylene blue from aqueous solutions by an adsorbent based on metal-organic framework and polyoxometalate, *J. Alloy. Comp.* 648 (2015) 986–993, <https://doi.org/10.1016/J.JALLCOM.2015.07.065>.
- H. Gupta, S. Roy, Geothermal Energy: A Alternative Resource for the 21st Century, 2007, <https://doi.org/10.1016/B978-0-444-52875-9.X5000-X>.
- R. Li, K.C. Chan, X.J. Liu, X.H. Zhang, L. Liu, T. Li, Z.P. Lu, Synthesis of well-aligned CuO nanowire array integrated with nanoporous CuO network for oxidative degradation of methylene blue, *Corros. Sci.* 126 (2017) 37–43, <https://doi.org/10.1016/J.CORUSCI.2017.06.001>.
- M. Zhu, D. Meng, C. Wang, J. Di, G. Diao, Degradation of methylene blue with H<sub>2</sub>O<sub>2</sub> over a cupric oxide nanosheet catalyst, *Chin. J. Catal.* 34 (2013) 2125–2129, [https://doi.org/10.1016/S1872-2067\(12\)60717-7](https://doi.org/10.1016/S1872-2067(12)60717-7).
- E. Haque, J.W. Jun, S.H. Jung, Adsorptive removal of methyl orange and methylene blue from aqueous solution with a metal-organic framework material, iron terephthalate (MOF-235), *J. Hazard Mater.* 185 (2011) 507–511, <https://doi.org/10.1016/J.JHAZMAT.2010.09.035>.
- X. Zhang, P. Zhang, Z. Wu, L. Zhang, G. Zeng, C. Zhou, Adsorption of methylene blue onto humic acid-coated Fe<sub>3</sub>O<sub>4</sub> nanoparticles, *Colloid. Surf. Physicochem. Eng. Asp.* 435 (2013) 85–90, <https://doi.org/10.1016/j.colsurfa.2012.12.056>.
- J. Ma, D. Huang, J. Zou, L. Li, Y. Kong, S. Komarneni, Adsorption of methylene blue and Orange II pollutants on activated carbon prepared from banana peel, *J. Porous Mater.* 22 (2015) 301–311, <https://doi.org/10.1007/s10934-014-9896-2>.
- R.F.P. Nogueira, A.G. Trovó, M.R.A. da Silva, R.D. Villa, M.C. de Oliveira, Fundamentos e aplicações ambientais dos processos fenton e foto-fenton, *Quim. Nova* 30 (2007) 400–408, <https://doi.org/10.1590/S0100-40422007000200030>.
- M.M.A. Raizada, D. Ganguly, A highly efficient copper oxide nanopowder for adsorption of methylene blue dye from aqueous medium, *J. Chem. Eng. Res.* 2 (2014) 249–258.
- F. Habe, J.W.R. The catalytic decomposition of hydrogen peroxide by iron salts, *Proc. R. Soc. London. Ser. A Math. Phys. Sci.* 147 (1934) 332–351, <https://doi.org/10.1098/rspa.1934.0221>.
- J.J. Pignatello, E. Oliveros, A. MacKay, Advanced oxidation processes for organic contaminant destruction based on the fenton reaction and related chemistry, *Crit. Rev. Environ. Sci. Technol.* 36 (2006) 1–84, <https://doi.org/10.1080/10643380500326564>.
- A.N. Pham, G. Xing, C.J. Miller, T.D. Waite, Fenton-like copper redox chemistry revisited: hydrogen peroxide and superoxide mediation of copper-catalyzed oxidant production, *J. Catal.* 301 (2013) 54–64, <https://doi.org/10.1016/J.JCAT.2013.01.025>.
- A. Xu, X. Li, S. Ye, G. Yin, Q. Zeng, Catalyzed oxidative degradation of methylene blue by in situ generated cobalt (II)-bicarbonate complexes with hydrogen peroxide, *Appl. Catal. B Environ.* 102 (2011) 37–43, <https://doi.org/10.1016/J.APCATB.2010.11.022>.
- N.A. Youssef, S.A. Shaban, F.A. Ibrahim, A.S. Mahmoud, Degradation of methyl orange using Fenton catalytic reaction, *Egypt. J. Petrol.* 25 (2016) 317–321, <https://doi.org/10.1016/J.EJPE.2015.07.017>.
- C. Walling, S. Kato, Oxidation of alcohols by Fenton's reagent. Effect of copper ion, *J. Am. Chem. Soc.* 93 (1971) 4275–4281, <https://doi.org/10.1021/ja00746a031>.
- K. Choi, W. Lee, Enhanced degradation of trichloroethylene in nano-scale zero-valent iron Fenton system with Cu(II), *J. Hazard Mater.* 211–212 (2012) 146–153, <https://doi.org/10.1016/J.JHAZMAT.2011.10.056>.
- C.L.P.S. Zanta, L.C. Friedrich, A. Machulek, K.M. Higa, F.H. Quina, Surfactant degradation by a catechol-driven Fenton reaction, *J. Hazard Mater.* 178 (2010) 258–263, <https://doi.org/10.1016/J.JHAZMAT.2010.01.071>.
- R. Valenzuela, D. Contreras, C. Oviedo, J. Freer, J. Rodríguez, Copper catechol-driven Fenton reactions and their potential role in wood degradation, *Int. Biodeterior. Biodegrad.* 61 (2008) 345–350, <https://doi.org/10.1016/J.IBIOD.2007.10.006>.
- S. Karthikeyan, M.P. Pachamuthu, M.A. Isaacs, S. Kumar, A.F. Lee, G. Sekaran, Cu and Fe oxides dispersed on SBA-15: a Fenton type bimetallic catalyst for N,N-diethyl-p-phenyl diamine degradation, *Appl. Catal. B Environ.* 199 (2016) 323–330, <https://doi.org/10.1016/j.apcatb.2016.06.040>.
- Y. Xue, S. Lu, X. Fu, V.K. Sharma, I. Mendoza-Sanchez, Z. Qiu, Q. Sui, Simultaneous removal of benzene, toluene, ethylbenzene and xylene (BTEX) by CuO<sub>2</sub> based Fenton system: enhanced degradation by chelating agents, *Chem. Eng. J.* 331 (2018) 255–264, <https://doi.org/10.1016/J.CEJ.2017.08.099>.
- J. Peng, J. Li, H. Shi, Z. Wang, S. Gao, Oxidation of disinfectants with Cl-substituted structure by a Fenton-like system Cu<sub>2</sub>+/H<sub>2</sub>O<sub>2</sub> and analysis on their structure-reactivity relationship, *Environ. Sci. Pollut. Res.* 23 (2016) 1898–1904, <https://doi.org/10.1007/s11356-015-5454-y>.
- S.P. Meshram, P.V. Adhyapak, U.P. Mulik, D.P. Amalnerkar, Facile synthesis of CuO nanomorphs and their morphology dependent sunlight driven photocatalytic properties, *Chem. Eng. J.* 204–206 (2012) 158–168, <https://doi.org/10.1016/J.CEJ.2012.07.012>.
- S. Dagher, Y. Haik, A.I. Ayesh, N. Tit, Synthesis and optical properties of colloidal CuO nanoparticles, *J. Lumin.* 151 (2014) 149–154, <https://doi.org/10.1016/J.JLUMIN.2014.02.015>.
- Z. Hong, Y. Cao, J. Deng, A convenient alcoholthermal approach for low temperature synthesis of CuO nanoparticles, *Mater. Lett.* 52 (2002) 34–38, [https://doi.org/10.1016/S0167-577X\(01\)00361-5](https://doi.org/10.1016/S0167-577X(01)00361-5).
- A. Angi, D. Sanli, C. Erkey, Ö. Bicer, Catalytic activity of copper (II) oxide prepared via ultrasound assisted Fenton-like reaction, *Ultrason. Sonochem.* 21 (2014) 854–859, <https://doi.org/10.1016/J.ULTSONCH.2013.09.006>.
- S.-H. Lee, Y.-S. Her, E. Matijević, Preparation and growth mechanism of uniform colloidal copper oxide by the controlled double-jet precipitation, *J. Colloid Interface Sci.* 186 (1997) 193–202, <https://doi.org/10.1006/JCIS.1996.4638>.
- N. Nasihat Sheno, A. Morsali, S. Woo Joo, Synthesis CuO nanoparticles from a copper(II) metal-organic framework precursor, *Mater. Lett.* 117 (2014) 31–33, <https://doi.org/10.1016/J.MATLET.2013.11.096>.
- E. Akbarzadeh, M. Falamarzi, M.R. Gholami, Synthesis of M/CuO (M = Ag, Au) from Cu based Metal Organic Frameworks for efficient catalytic reduction of p-nitrophenol, *Mater. Chem. Phys.* 198 (2017) 374–379, <https://doi.org/10.1016/J.MATCHEMPHYS.2017.06.022>.
- P. Arul, S. Abraham John, Electrodeposition of CuO from Cu-MOF on glassy carbon electrode: a non-enzymatic sensor for glucose, *J. Electroanal. Chem.* 799 (2017) 61–69, <https://doi.org/10.1016/J.JELECHEM.2017.05.041>.
- H.-J. Peng, G.-X. Hao, Z.-H. Chu, C.-L. He, X.-M. Lin, Y.-P. Cai, Mesoporous spindle-like hollow CuO/C fabricated from a Cu-based metal-organic framework as anodes for high-performance lithium storage, *J. Alloy. Comp.* 727 (2017) 1020–1026, <https://doi.org/10.1016/J.JALLCOM.2017.08.231>.
- B.S. Barros, O.J. deLima Neto, A.C. deOliveiraFrós, J. Kulesza, Metal-organic framework nanocrystals, *Chemistry* 3 (2018) 7459–7471, <https://doi.org/10.1002/slct.201801423>.
- A. Aslami, A. Morsali, M. Zeller, Nano-structures of two new lead(II) coordination polymers: new precursors for preparation of PbS nano-structures, *Solid State Sci.* 10 (2008) 1591–1597, <https://doi.org/10.1016/J.SOLIDSTATESCIENCES.2008.02.012>.
- M.Y. Masoomi, A. Morsali, Applications of metal-organic coordination polymers as precursors for preparation of nano-materials, *Coord. Chem. Rev.* 256 (2012) 2921–2943, <https://doi.org/10.1016/J.CCR.2012.05.032>.

- [34] A.M. Joaristi, J. Juan-alcan, P. Serra-crespo, F. Kapteijn, J. Gascon, Electrochemical synthesis of some archetypical Zn<sup>2+</sup>, Cu<sup>2+</sup>, and Al<sup>3+</sup> metal organic frameworks, *Cryst. Growth Des.* 12 (2012) 3489–3498, <https://doi.org/10.1021/cg300552w>.
- [35] J. Kulesza, B.S. Barros, I.M.V. da Silva, G.G. da Silva, S. Alves Júnior, Efficient and environmentally friendly electrochemical synthesis of the metallacalixarene [Cu(1,3-bdc)-DMF]·2H<sub>2</sub>O, *CrystEngComm* 15 (2013) 8881–8882, <https://doi.org/10.1039/c3ce41679h>.
- [36] O.J. de Lima Neto, A.C. de O. Frós, B.S. Barros, A.F. de Farias Monteiro, J. Kulesza, Rapid and efficient electrochemical synthesis of a zinc-based nano-MOF for Ibuprofen adsorption, *New J. Chem.* 43 (2019) 5518–5524, <https://doi.org/10.1039/C8NJ06420B>.
- [37] H.K. Lee, D.-W. Min, B.-Y. Cho, S.W. Lee, Two-dimensional copper coordination polymers based on paddle-wheel type secondary building units of Cu<sub>2</sub>(CO<sub>2</sub>R)<sub>4</sub>: [Cu(1,3-BDC)(H<sub>2</sub>O)]·2H<sub>2</sub>O and [Cu<sub>2</sub>(OBC)<sub>2</sub>(H<sub>2</sub>O)<sub>2</sub>]·H<sub>2</sub>O (1,3-BDC = 1,3-benzenedicarboxylate; OBC = 4,4'-oxybis(benzoate)), *Bull. Korean Chem. Soc.* 25 (2004) 1955–1958, <https://doi.org/10.5012/bkcs.2004.25.12.1955>.
- [38] J. Liu, B. Lukose, O. Shekhah, H.K. Arslan, P. Weidler, H. Gliemann, S. Bräse, S. Grosjean, A. Godt, X. Feng, K. Müllen, I.-B. Magdau, T. Heine, C. Wöll, A novel series of isorecticular metal organic frameworks: realizing metastable structures by liquid phase epitaxy, *Sci. Rep.* 2 (2012) 1–5, <https://doi.org/10.1038/srep00921>.
- [39] Y. Shen, Z. Zhang, K. Xiao, Evaluation of cobalt oxide, copper oxide and their solid solutions as heterogeneous catalysts for Fenton-degradation of dye pollutants, *RSC Adv.* 5 (2015) 91846–91854, <https://doi.org/10.1039/C5RA18923C>.
- [40] P. Deka, A. Hazarika, R.C. Deka, P. Bharali, Influence of CuO morphology on the enhanced catalytic degradation of methylene blue and methyl orange, *RSC Adv.* 6 (2016) 95292–95305, <https://doi.org/10.1039/C6RA20173C>.
- [41] A. Tabaï, O. Bechiri, M. Abbessi, Degradation of organic dye using a new homogeneous Fenton-like system based on hydrogen peroxide and a recyclable Dawson-type heteropolyanion, *Int. J. Ind. Chem.* 8 (2017) 83–89, <https://doi.org/10.1007/s40090-016-0104-x>.
- [42] A. Salhi, A. Aarfane, S.M. Tahiri, L. Khamliche, M. Bensitel, F. Bentiss, M. El Krati, Study of the photocatalytic degradation of methylene blue dye using titanium-doped hydroxyapatite, *Mediterr. J. Chem.* 4 (2015) 59–67, <https://doi.org/10.13171/mjc.4.1.2015.16.01.20.30/salhi>.
- [43] J.-H. Sun, S.-H. Shi, Y.-F. Lee, S.-P. Sun, Fenton oxidative decolorization of the azo dye Direct Blue 15 in aqueous solution, *Chem. Eng. J.* 155 (2009) 680–683, <https://doi.org/10.1016/J.CEJ.2009.08.027>.
- [44] M.U. Anu Prathap, B. Kaur, R. Srivastava, Hydrothermal synthesis of CuO micro-/nanostructures and their applications in the oxidative degradation of methylene blue and non-enzymatic sensing of glucose/H<sub>2</sub>O<sub>2</sub>, *J. Colloid Interface Sci.* 370 (2012) 144–154, <https://doi.org/10.1016/J.JCIS.2011.12.074>.
- [45] M. Yang, J. He, Fine tuning of the morphology of copper oxide nanostructures and their application in ambient degradation of methylene blue, *J. Colloid Interface Sci.* 355 (2011) 15–22, <https://doi.org/10.1016/J.JCIS.2010.11.022>.